

Sunspots rotation and magnetic transients associated with flares in NOAA AR 11429 *

Jianchuan Zheng¹, Zhiliang Yang¹, Jianpeng Guo^{1,2}, Kaiming Guo¹, Hui Huang¹, Xuan Song¹ and Weixing Wan^{2,3}

¹ Department of Astronomy, Beijing Normal University, Beijing 100875, China;
zhengjc@mail.bnu.edu.cn, jpguo@bnu.edu.cn

² Key Laboratory of Earth and Planetary Physics, Institute of Geology and Geophysics, Chinese Academy of Sciences, Beijing 100029, China

³ College of Earth Sciences, University of Chinese Academy of Sciences, Beijing, China

Received —; accepted —

Abstract We analyze sunspots rotation and magnetic transients in NOAA AR 11429 during two X-class (X5.4 and X1.3) flares using the data from the Helioseismic and Magnetic Imager on board the *Solar Dynamics Observatory*. A large leading sunspot with positive magnetic polarity rotated counterclockwise. As expected, the rotation was significantly affected by the two flares. The magnetic transients induced by the flares were clearly evident in the sunspots with negative polarity. They were moving across the sunspots with speed of order $3 - 7 \text{ km s}^{-1}$. Furthermore, the trend of magnetic flux evolution of these sunspots exhibited changes associated with the flares. These results may shed light on the understanding of the evolution of sunspots.

Key words: Sunspots; Sun: rotation; Sun: magnetic fields

1 INTRODUCTION

Sunspots are concentrations of strong magnetic field on the solar surface, consisting of a dark umbra and a fibrous penumbra (Solanki 2003). It is generally accepted that eruption events such as flares occurring in upper atmosphere are associated with magnetic field generated from the base of convection zone, emerging as bipolar magnetic regions at solar surface, then extending to corona (Solanki et al. 2006). So the visible sunspots play an important role in studying a variety of phenomena on the Sun.

The evolution of sunspots includes formation, movement, deformation and disappearance. Rotation is an important feature during evolution. In general, there are two kinds of rotation: one sunspot rotates around its umbral centre and one sunspot rotates around the other (Yan & Qu 2012). The rotation of sunspots and spot-groups have been studied for many decades (see, e.g., Evershed 1910; St. John 1913; Maltby 1964; Brown et al. 2003; Zhang et al. 2007; Yan et al. 2009; Min & Chae 2009). Yan et al. (2008b) found 182 significantly rotating sunspots among 2959 active regions. Some authors believed the rotational motion of sunspots may be involved with energy build-up and later release by flares (e.g., Stenflo 1969; Barnes & Sturrock 1972; Hiremath et al. 2005; Zhang et al. 2008). Furthermore, the relationships between the sunspot rotation and coronal consequence (Brown et al. 2003; Tian et al. 2008), flare productivity (Yan et al. 2008a; Zhang et al. 2008; Ruan et al. 2014), direction of the rotation (Zheng et al. 2016), and magnetic helicities (Vemareddy et al. 2012) have been investigated. The association of

* Supported by the National Natural Science Foundation of China.

flares with abnormal rotation rates (Hiremath et al. 2005) has been found. Specifically, Wang et al. (2014) reported two sunspots in AR 11158 rotating along with a X2.2 flare. Liu et al. (2016) reported a non-uniform rotation induced by a M6.5 flare in NOAA AR 12371, and Bi et al. (2016) found an abrupt reverse rotation of sunspot in NOAA AR 12158 caused by back reaction of X1.6 flare.

Besides, the photospheric magnetic field changes during the flares. The magnetic field is distorted enough to store energy powering flare. After a flare taking place, the distorted field relax and restructure (Sakurai & Hiei 1996). There are two kinds of changes of magnetic field based on observations: the first is rapid short-term changes (Patterson & Zirin 1981; Zhao et al. 2009), which is due to flare-induced spectral line changes (Patterson 1984; Qiu & Gary 2003). It is generally believed that the rapid short-term changes are not the real changes of magnetic field (see, Ding et al. 2002). However, Harker & Pevtsov (2013) also analyzed the magnetic transients during the M7.9 flare in NOAA AR 11429 on 13 March 2012 and suggested that the magnetic transients represented a real change in the photospheric magnetic field. Another is irreversible changes from pre-flare to post-flare (e.g., Spirock et al. 2002; Wang et al. 2002; Wang 2006; Song & Zhang 2016). The irreversible changes were first noticed by Wang et al. (1994). They showed that magnetic shear increased after flares with vector magnetic field data. Cameron & Sammis (1999) reported a change in the line-of-sight (LOS) field during the X9.3 flare on 24 May 1990 with the videomagnetograph data from the Big Bear Solar Observatory (BBSO). Sudol & Harvey (2005) and Petrie & Sudol (2010) analyzed the changes of the LOS magnetic field during some X- and M- class flares with Global Oscillation Network Group (GONG) magnetograms. The median duration of changes was about 15 minutes and the median absolute value of changes was about 69 G. Wang & Liu (2010) demonstrated that the change of LOS magnetic field is due to increase of horizontal magnetic field near the polarity inversion line. With the seeing-free data of vector magnetograms, Liu et al. (2012) found that the photospheric transverse magnetic field enhancement was associated with the M6.6 flare in NOAA AR 11158. Wang et al. (2012) observed the same phenomenon associated with the X2.2 flare in this active region. These results suggested that the magnetic field near the polarity inversion line could become more horizontal after a flare.

In this study, we analyze the evolution of sunspots in NOAA AR 11429. We will explore the rotation of sunspots along with the flares, i.e., how do the flares and the rotation of sunspots affect each other. The magnetic transients induced by flares are studied in prior works. We further study the motion of the magnetic transients to understand how the flares influence sunspots. The paper is organized as follows. In Section 2 we describe the data used and the entire structure of the active region. Section 3 shows data processing. We summarize and discuss the results in Section 4.

2 OBSERVATIONAL DATA

The 45 s cadence and spatial sampling of $0''.5 \text{ pixel}^{-1}$ full-disk continuum intensity images and line-of-sight magnetograms observed by the Helioseismic and Magnetic Imager (HMI; Schou et al. 2012) on board the *Solar Dynamics Observatory* (*SDO*) are used to analyze the variation of sunspots in NOAA AR 11429. The images from the Atmospheric Imaging Assembly (AIA; Lemen et al. 2012) on board *SDO* are used to investigate the chromospheric and coronal context: AIA 304 Å formed in transition region and chromosphere, and AIA 1600 Å formed in upper photosphere and transition region.

AR 11429 appeared on the eastern limb on 3 March 2012, and then rapidly became complicated reverse-polarity $\beta\gamma\delta$ active region. The evolution and development of AR 11429 from 5 March to 12 March are displayed in Figure 1. It is interesting to note that the sunspots in this active region were moving away from each other, i.e., the leading sunspots moving westward and the following sunspots moving eastward. Several major eruptions were clearly visible in this active region. Typically, three X-class flares occurred: one (X1.1) on 5 March and two of interest (X5.4 and X1.3) on 7 March. The GOES soft X-ray flux (Figure 3a) indicates that the X5.4 flare started at 00:02 UT, peaked at 00:27 UT, and ended at 00:40 UT, and the X1.3 flare started at 01:05 UT, peaked at 01:14 UT, and ended at 01:23 UT. The evolution of five prominent sunspots, two positive polarity sunspots (P1 and P2) and three negative polarity sunspots (N1, N2 and N3), were associated with these two flares, as be discussed in the next section.

3 ANALYSIS AND RESULTS

3.1 Sunspots rotating associated with flares

To study the rotation, we take the rotation of individual sunspots as a simplified solid-body rotation (i.e., a sunspot rotates around its umbral center), and track the variation of the ellipses that best fit individual sunspots on time-series intensity images (see [Bi et al. 2016](#)). Take sunspot P1 as an example. The best-fit ellipses on the intensity images at 23:29:23 UT of 6 March and 01:28:38 UT of 7 March are shown in Figure 2(a) and Figure 2(b), respectively. Obviously, the major axis rotates counterclockwise about 7° . In the present study, the changes of the angle between the major axis and the horizontal direction of the best-fit ellipses are used to describe the rotation of the sunspot. The results together with the GOES soft X-ray flux are shown in Figure 3.

Figure 3(b) shows that P1 rotated mainly counterclockwise from $\sim 23:30$ UT of 6 March to $\sim 01:30$ UT of 7 March. Before the start of the X5.4 flare, the rotation was very fast with speed up to $7.92^\circ \text{ hr}^{-1}$. From start to peak of the flare, the rotation speed decreased slowly to about $4.89^\circ \text{ hr}^{-1}$ and the rotation trend kept counterclockwise. Just after the peak of the flare, the rotation trend reversed from counterclockwise to clockwise. Its speed was about $4.07^\circ \text{ hr}^{-1}$. After the flare, the rotation direction returned to counterclockwise with the rotation speed of about $6.56^\circ \text{ hr}^{-1}$, and the rotation speed increased gradually until the beginning of the X1.3 flare. Later, the rotation trend reversed to clockwise again with the rotation speed of about $6.44^\circ \text{ hr}^{-1}$ and slowed down. These results indicate that the rotation of sunspot P1 was significantly affected by both flares. The relative mean intensity profiles in different AIA wavelengths, obtained from the co-aligned with HMI images, are also plotted in Figure 3. The intensity in the AIA wavelengths of 304 \AA (green curve) and AIA 1600 \AA (blue curve) started rising around 00:05 UT, peaked at about 00:07 UT, and then decreased during the impulsive phase of the X5.4 flare. At about 01:05 UT, the intensities started rising again and peaked at about 01:14 UT. It provides further support for the view that solar flares are often related to the rotation of sunspots.

The rotation of the sunspot N1 was complicated (Figure 3c). Before the peak of the X5.4 flare, the rotation trend was mainly counterclockwise, and then reversed to clockwise. The situation around the X1.3 flare was similar to that around the former flare. The intensity of AIA wavelengths increased and the rotation changed significantly during the impulsive phases of the X5.4 and X1.3 flares. As shown in Figure 3(d), sunspot N2 rotated clockwise from $\sim 00:15$ UT to $\sim 00:40$ UT. The relative mean intensity of 1600 \AA in this sunspot started rising at $\sim 00:05$ UT and reached its maximum at $\sim 00:20$ UT. The relative mean intensity of 304 \AA started rising at $\sim 00:05$ UT and reached its maximum at $\sim 00:30$ UT. So the X5.4 flare affected the rotation of sunspot N2. The sunspot N3 remained stable during the two flares (Figure 3e). The rotation speed was poorly correlated with the intensity of AIA wavelengths, and therefore the X5.4 and X1.3 flares.

3.2 The motion of Magnetic Transient

Magnetic transients induced by flares have been well investigated by [Patterson \(1984\)](#) and [Qiu & Gary \(2003\)](#). They analyzed the cause, location and level of the magnetic transients. Here, we find that there are some magnetic transients moving through sunspots N1, N2 and N3, and there is no apparent magnetic transient motion in the sunspots P1 and P2. Because the polarity of the sunspots N1, N2 and N3 is negative (black regions in the magnetograms), the magnetic transients means that the polarity is reversed.

Figure 4 shows the changes of the magnetic field in sunspot N1. At 01:09 UT of 7 March, the magnetic transients marked by red arrows in the umbra of the sunspot can be clearly seen. These magnetic transients (the positive magnetic field) moved toward the southeast direction. At 01:14 UT, the area with positive magnetic field became larger while the strength became weaker, as shown in Figure 4(a2). The green line in Figure 4(a3) indicates the moving trajectory of the positive polarity points. To investigate the kinematic evolution of the reversed polarity, the time-distance plots obtained along the green trajectory line are shown in Figure 4(d). A white streak is clearly visible. It started at $\sim 01:07$ UT and ended at

~01:16 UT, consistent with the time of the X1.3 flare. It might imply that the reversed magnetic polarity was caused by this flare. The distance corresponding to the streak was about 5 arcsec. Thus, the moving speed of the magnetic transients can be estimated to be about 6.59 km s^{-1} . Similarly, some magnetic transients (i.e., the reversed magnetic field) were presented in sunspots N2 and N3, and probably associated with the X5.4 flare, as shown in Figures 5 and 6. They were moving toward southeast with speed about 3.69 km s^{-1} and 3.22 km s^{-1} respectively.

In order to check whether the magnetic transients were co-spatial with flare ribbons, we further examined the co-aligned AIA 304 Å and AIA 1600 Å images corresponding to HMI magnetograms, which are displayed in panels (b1)–(b3) and panels (c1)–c(3) in Figures 4, 5 and 6 respectively. The flare ribbons can be seen in these panels. They were separating from each other. The locations of sunspots N1, N2 and N3 in AIA images, marked by magnetogram contours at -800 G, were moving with flare ribbons. This implies the magnetic transients were co-spatial with flare ribbons.

We calculated magnetic flux of sunspots N1, N2 and N3 for the regions marked by the red rectangular boxes in Figure 1. The magnetic flux of sunspots with negative polarity together with GOES soft X-ray flux are shown in Figure 7. Before the start of the X5.4 flare, the absolute value of magnetic flux in sunspot N1 decreased slowly. From the start to peak of the flare, it decreased gradually. Then, the value kept almost unchanged. At the end of the flare, it increased slightly. During the period of the X1.3 flare, the absolute value of magnetic flux decreased first and then increased abruptly. These results suggest that the changes of trend of magnetic flux in sunspot N1 were caused by both the X5.4 flare and the X1.3 flare.

The magnetic flux of sunspot N2 mainly increased from 23:30 UT of 6 March to 01:30 UT of 7 March. There was an obvious change near the peak of X5.4 flare. Specifically, the absolute value decreased first and then increased, as shown in Figure 7(c). The absolute magnetic flux value of sunspot N3 (Figure 7d) almost kept unchanged before the start of the X5.4 flare. Similarly, during the X5.4 flare, the magnetic flux decreased rapidly, and then increased monotonically. These results suggest that the changes of trend of magnetic flux in sunspots N2 and N3 were mainly due to the X5.4 flare.

4 SUMMARY AND DISCUSSION

AR 11429 is a complicated active region with a reversed polarity structure, in contrast with the nature of solar cycle 24. It has a large leading sunspot with positive magnetic polarity (P1) exhibiting significant counterclockwise rotation. The rotation underwent some changes during two X-class (X5.4 and X1.3) flares. It is possible that the flares were triggered by the sunspot rotation (see Zhang et al. 2008; Vemareddy et al. 2016), and in turn they reacted back and affected the sunspot P1 rotation.

The magnetic transients induced by the two X-class flares can be seen in sunspots with negative magnetic polarity (N1, N2 and N3). They moved outward with respect to the center of the active region and moved through the sunspots quickly with speed up to about 6.59 km s^{-1} . The magnetic transients lasted for about ten minutes within the period of the X5.4 and X1.3 flare. As expected, the magnetic transients, which are clearly illustrated in sunspots N1, N2 and N3 were moving away from the polarity inversion line shown in Figures 4, 5 and 6. The magnetic transients occurred during the X5.4 and X1.3 flares were co-spatial with flare ribbons. This is consistent with Maurya et al. (2012), who found that magnetic transients in AR 11158 during a X2.2 flare persisted for a few minutes and showed co-spatial with flare ribbons, which were separating out with a mean velocity of 8 km s^{-1} .

During the evolution of sunspots (N1, N2 and N3), changes in the trend of magnetic field evolution were presented, and are associated with the two X-class flares. Similar results in five δ sunspots were found by Wang (2006). The increasing and decreasing tendency of the magnetic flux in active region might be attributed to magnetic flux emergence and magnetic cancellation (van Driel-Gesztelyi & Green 2015).

The evolution of sunspots with complicated structure can be affected by many factors such as interaction among sunspots within same active region, physical change induced by flare, and interaction between magnetic field and plasma. In this study, we have found that the motion and the trend of mag-

netic field evolution of sunspots are significantly affected by flares. Other influences on the evolution of sunspots will be examined in future studies.

Acknowledgements The authors thank the referees for their corrections and valuable suggestions to improve the paper. This work is supported by the National Natural Science Foundations of China (41231068, 41374187, 41531073, and 41674147). We acknowledge the *SDO/HMI* and *SDO/AIA* teams for providing the data. The GOES soft X-ray flux data is available at NASA/GSFC Solar Data Analysis Center (SDAC).

References

- Barnes, C. W., & Sturrock, P. A. 1972, *ApJ*, 174, 659 1
- Bi, Y., Jiang, Y., Yang, J., et al. 2016, *Nature Communications*, 7, 13798 2, 3
- Brown, D. S., Nightingale, R. W., Alexander, D., et al. 2003, *Sol. Phys.*, 216, 79 1
- Cameron, R., & Sammis, I. 1999, *ApJ*, 525, L61 2
- Ding, M. D., Qiu, J., & Wang, H. 2002, *ApJ*, 576, L83 2
- Evershed, J. 1910, *MNRAS*, 70, 217 1
- Harker, B. J., & Pevtsov, A. A. 2013, *ApJ*, 778, 175 2
- Hiremath, K. M., Suryanarayana, G. S., & Lovely, M. R. 2005, *A&A*, 437, 297 1, 2
- Lemen, J. R., Title, A. M., Akin, D. J., et al. 2012, *Sol. Phys.*, 275, 17 2
- Liu, C., Deng, N., Liu, R., et al. 2012, *ApJ*, 745, L4 2
- Liu, C., Xu, Y., Cao, W., et al. 2016, *Nature Communications*, 7, 13104 2
- Maltby, P. 1964, *Astrophysica Norvegica*, 8, 205 1
- Maurya, R. A., Vemareddy, P., & Ambastha, A. 2012, *ApJ*, 747, 134 4
- Min, S., & Chae, J. 2009, *Sol. Phys.*, 258, 203 1
- Patterson, A. 1984, *ApJ*, 280, 884 2, 3
- Patterson, A., & Zirin, H. 1981, *ApJ*, 243, L99 2
- Petrie, G. J. D., & Sudol, J. J. 2010, *ApJ*, 724, 1218 2
- Qiu, J., & Gary, D. E. 2003, *ApJ*, 599, 615 2, 3
- Ruan, G., Chen, Y., Wang, S., et al. 2014, *ApJ*, 784, 165 1
- Sakurai, T., & Hiei, E. 1996, *Advances in Space Research*, 17 2
- Schou, J., Scherrer, P. H., Bush, R. I., et al. 2012, *solphys*, 275, 229 2
- Solanki, S. K. 2003, *A&A Rev.*, 11, 153 1
- Solanki, S. K., Inhester, B., & Schüssler, M. 2006, *Reports on Progress in Physics*, 69, 563 1
- Song, Y. L., & Zhang, M. 2016, *ApJ*, 826, 173 2
- Spirock, T. J., Yurchyshyn, V. B., & Wang, H. 2002, *ApJ*, 572, 1072 2
- St. John, C. E. 1913, *ApJ*, 37, 322 1
- Stenflo, J. O. 1969, *Sol. Phys.*, 8, 115 1
- Sudol, J. J., & Harvey, J. W. 2005, *ApJ*, 635, 647 2
- Tian, L., Alexander, D., & Nightingale, R. 2008, *ApJ*, 684, 747 1
- van Driel-Gesztelyi, L., & Green, L. M. 2015, *Living Reviews in Solar Physics*, 12, 1 4
- Vemareddy, P., Ambastha, A., Maurya, R. A., & Chae, J. 2012, *ApJ*, 761, 86 1
- Vemareddy, P., Cheng, X., & Ravindra, B. 2016, *ApJ*, 829, 24 4
- Wang, H. 2006, *ApJ*, 649, 490 2, 4
- Wang, H., Ewell, Jr., M. W., Zirin, H., & Ai, G. 1994, *ApJ*, 424, 436 2
- Wang, H., & Liu, C. 2010, *ApJ*, 716, L195 2
- Wang, H., Spirock, T. J., Qiu, J., et al. 2002, *ApJ*, 576, 497 2
- Wang, S., Liu, C., Deng, N., & Wang, H. 2014, *ApJ*, 782, L31 2
- Wang, S., Liu, C., Liu, R., et al. 2012, *ApJ*, 745, L17 2
- Yan, X. L., & Qu, Z. Q. 2012, in *EAS Publications Series*, Vol. 55, *EAS Publications Series*, ed. M. Faurobert, C. Fang, & T. Corbard, 137 1
- Yan, X.-L., Qu, Z.-Q., & Kong, D.-F. 2008a, *MNRAS*, 391, 1887 1

- Yan, X. L., Qu, Z. Q., & Xu, C. L. 2008b, *ApJ*, 682, L65 [1](#)
- Yan, X.-L., Qu, Z.-Q., Xu, C.-L., Xue, Z.-K., & Kong, D.-F. 2009, *Research in Astronomy and Astrophysics*, 9, 596 [1](#)
- Zhang, J., Li, L., & Song, Q. 2007, *ApJ*, 662, L35 [1](#)
- Zhang, Y., Liu, J., & Zhang, H. 2008, *Sol. Phys.*, 247, 39 [1](#), [4](#)
- Zhao, M., Wang, J.-X., Matthews, S., et al. 2009, *Research in Astronomy and Astrophysics*, 9, 812 [2](#)
- Zheng, J., Yang, Z., Guo, K., Wang, H., & Wang, S. 2016, *ApJ*, 826, 6 [1](#)

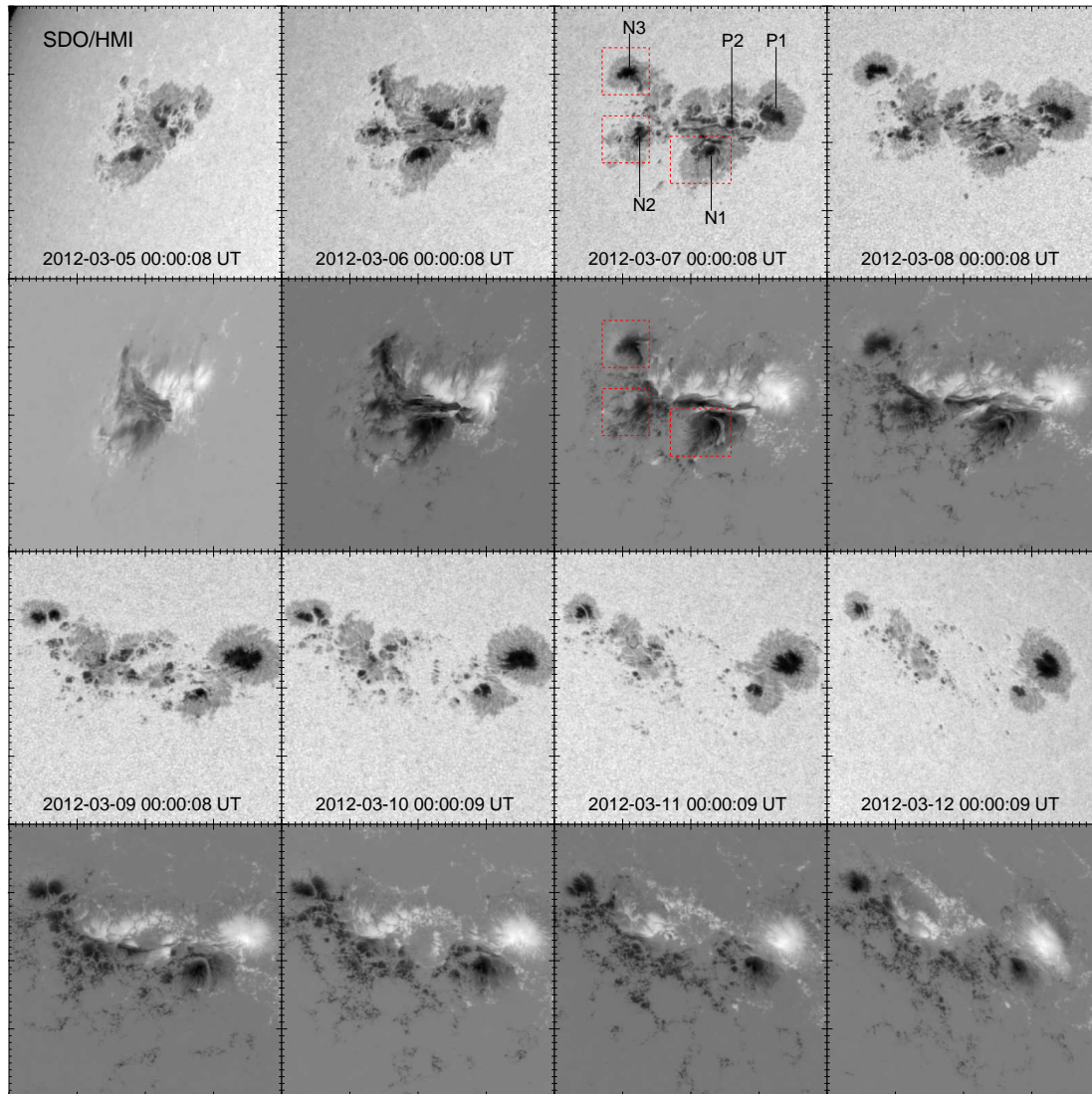


Fig. 1 The HMI intensity images and magnetograms show the evolution of AR 11429 during 5 - 12 March 2012. The field of view is $200'' \times 200''$. The main sunspots are labeled with P/N*. The white/black areas in magnetograms represent positive/negative magnetic polarity. The red rectangular boxes are the selected regions for further study.

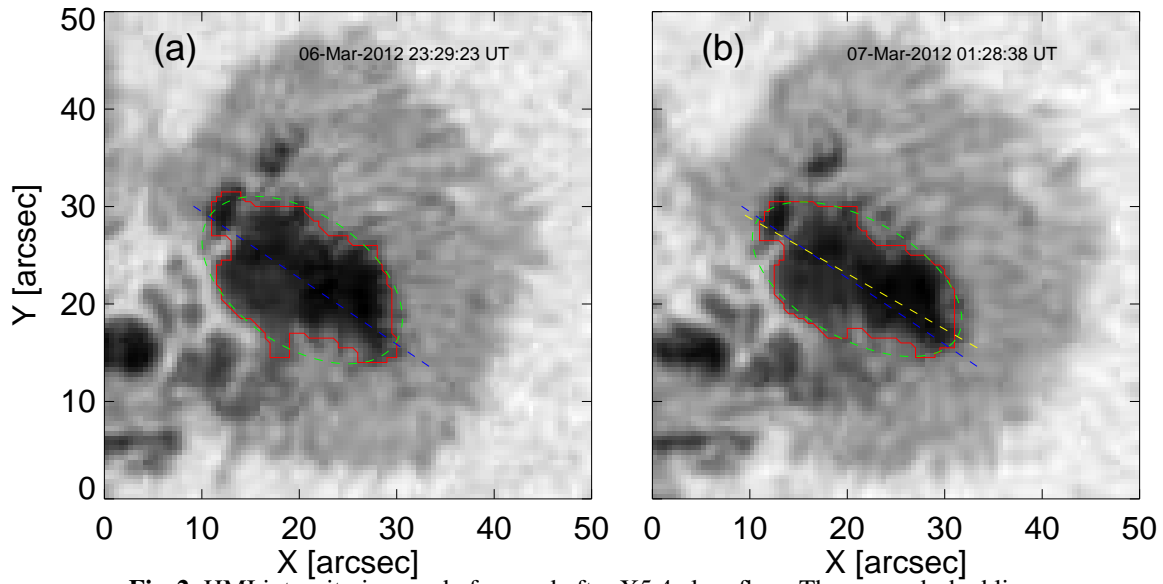


Fig. 2 HMI intensity images before and after X5.4 class flare. The green dashed lines represent the ellipse fit to the sunspots P1. The blue and yellow dashed lines are the major axes of the ellipses.

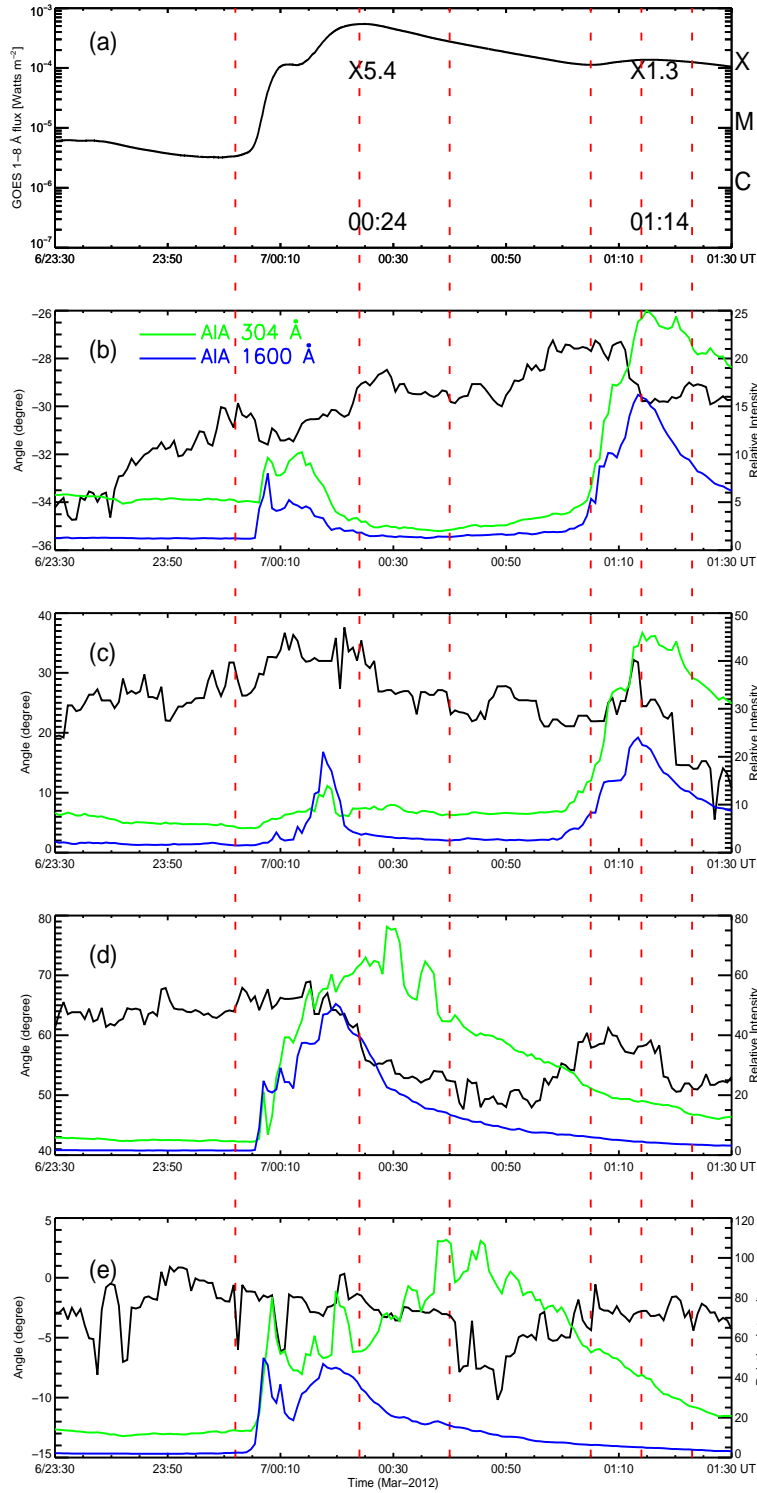


Fig. 3 (a) Evolution of GOES soft X-ray emission from 23:30 UT on 6 March to 01:30 UT on 7 March. The vertical dash lines represent the GOES flare start, peak and end times. (b)–(e) Time profiles of orientation angle (between the major axis and horizontal direction) of sunspot P1, N1, N2 and N3, respectively. The green and blue curves are profiles of relative mean intensity within each sunspot region with respect to the quiet Sun in AIA 304 Å and AIA 1600 Å respectively.

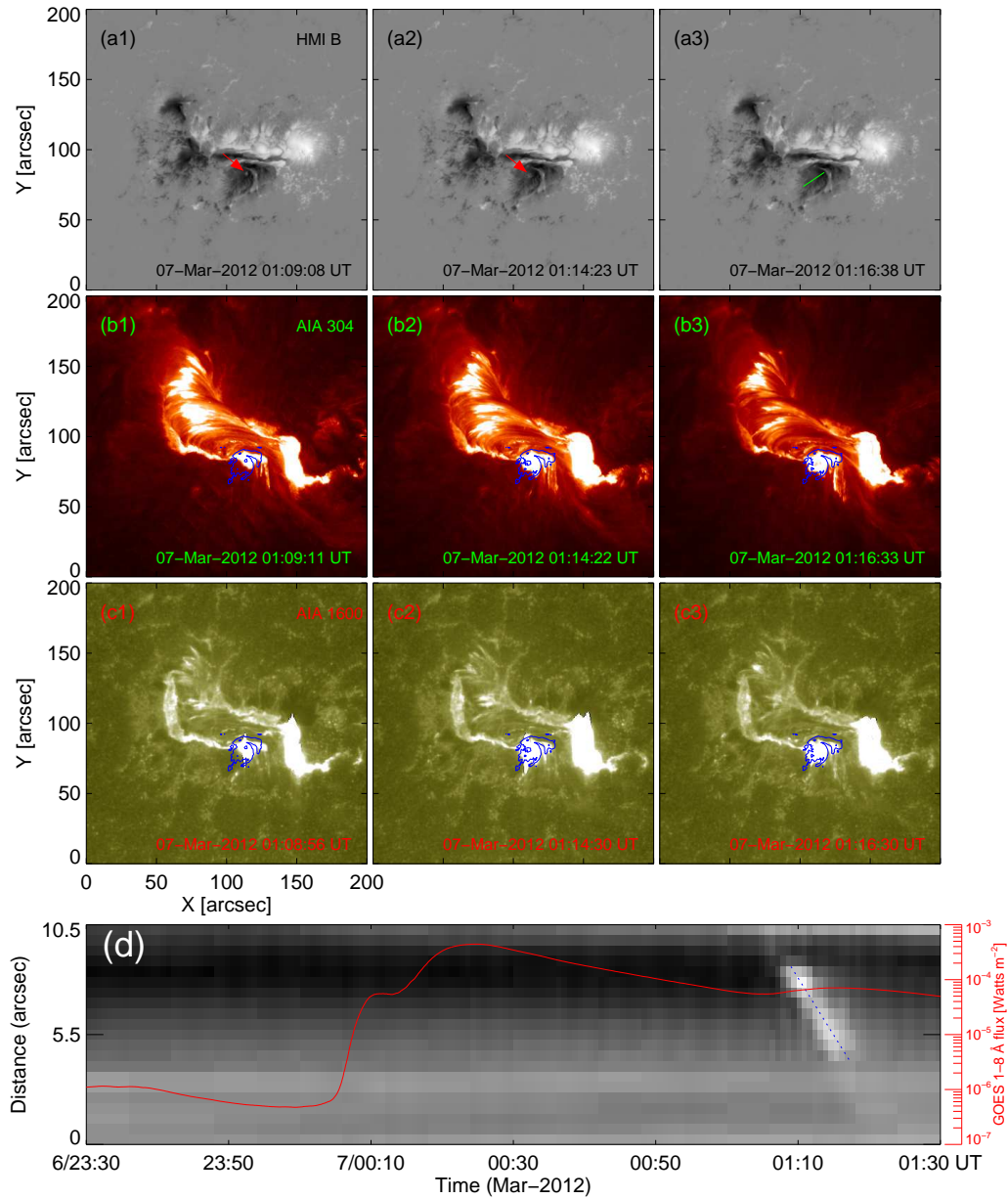


Fig. 4 The reversed magnetic field moving through sunspot N1. The red arrows in (a1) and (a2) indicate the location of the reversed magnetic field and the green line in (a3) indicates the trajectory of the moving reversed magnetic field. (b1)–(b3) The co-aligned AIA 304 Å images corresponding to HMI magnetograms. The blue contours represent the magnetic field of sunspot N1 at -800 G. (c1)–(c3) The co-aligned AIA 1600 Å images overlaid by magnetogram contours of sunspot N1. (d) Time-slice plot of the trajectory. The blue dashed line shows the evolution of the reversed magnetic field. The red curve overlaid on the time-slice plot is the GOES soft X-ray flux.

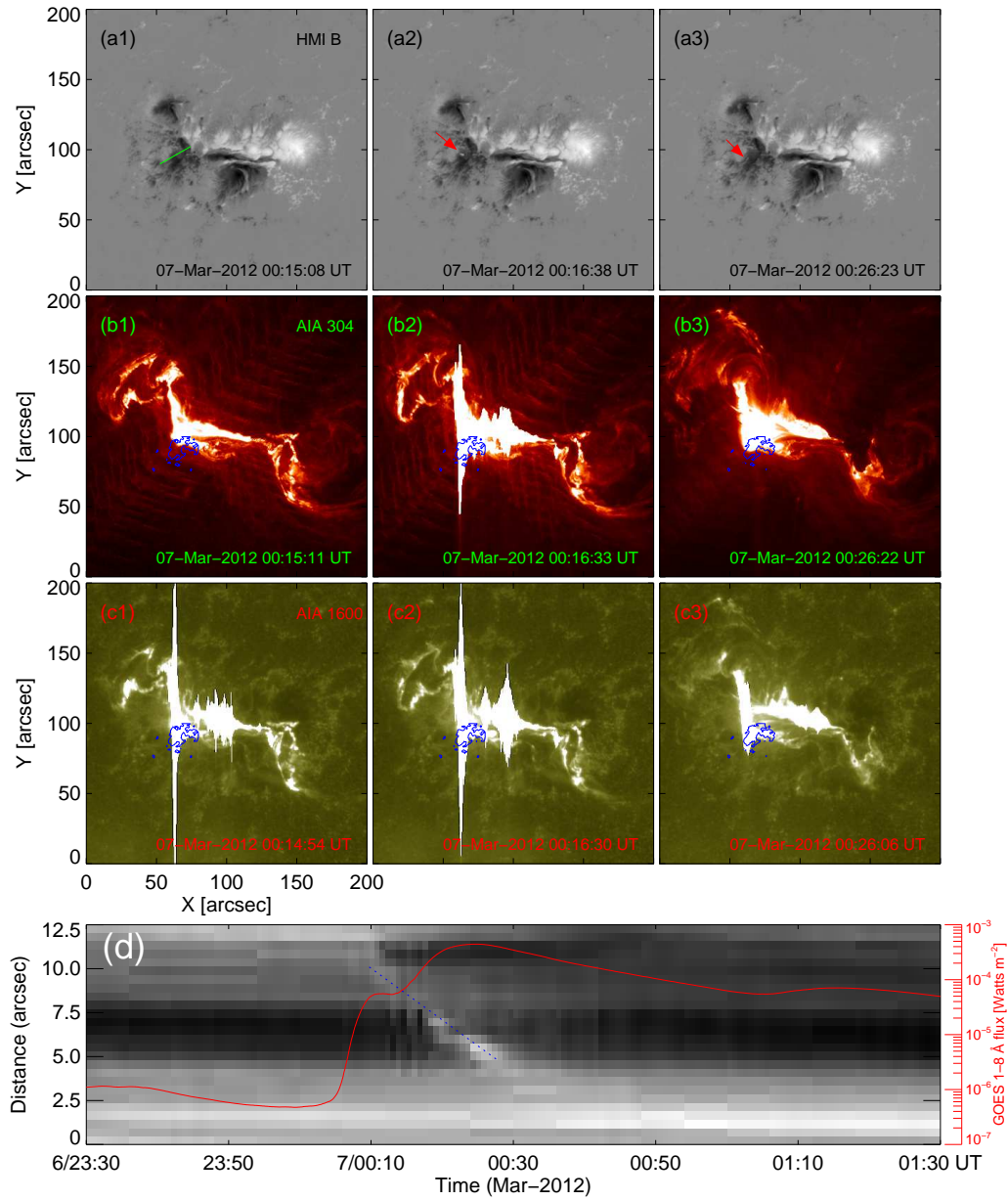


Fig. 5 Same as Figure 4, but for sunspot N2.

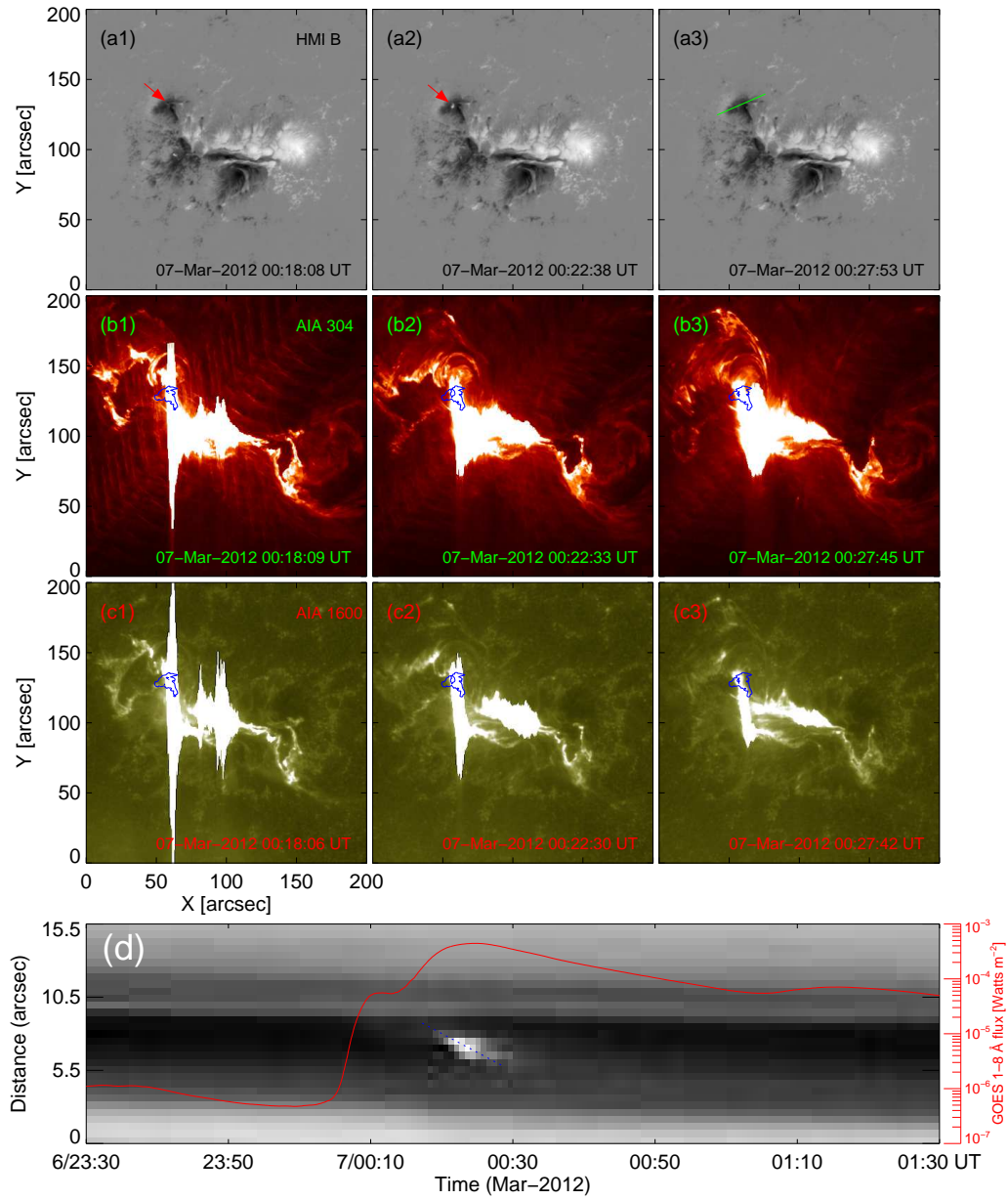


Fig. 6 Same as Figure 4, but for sunspot N3.

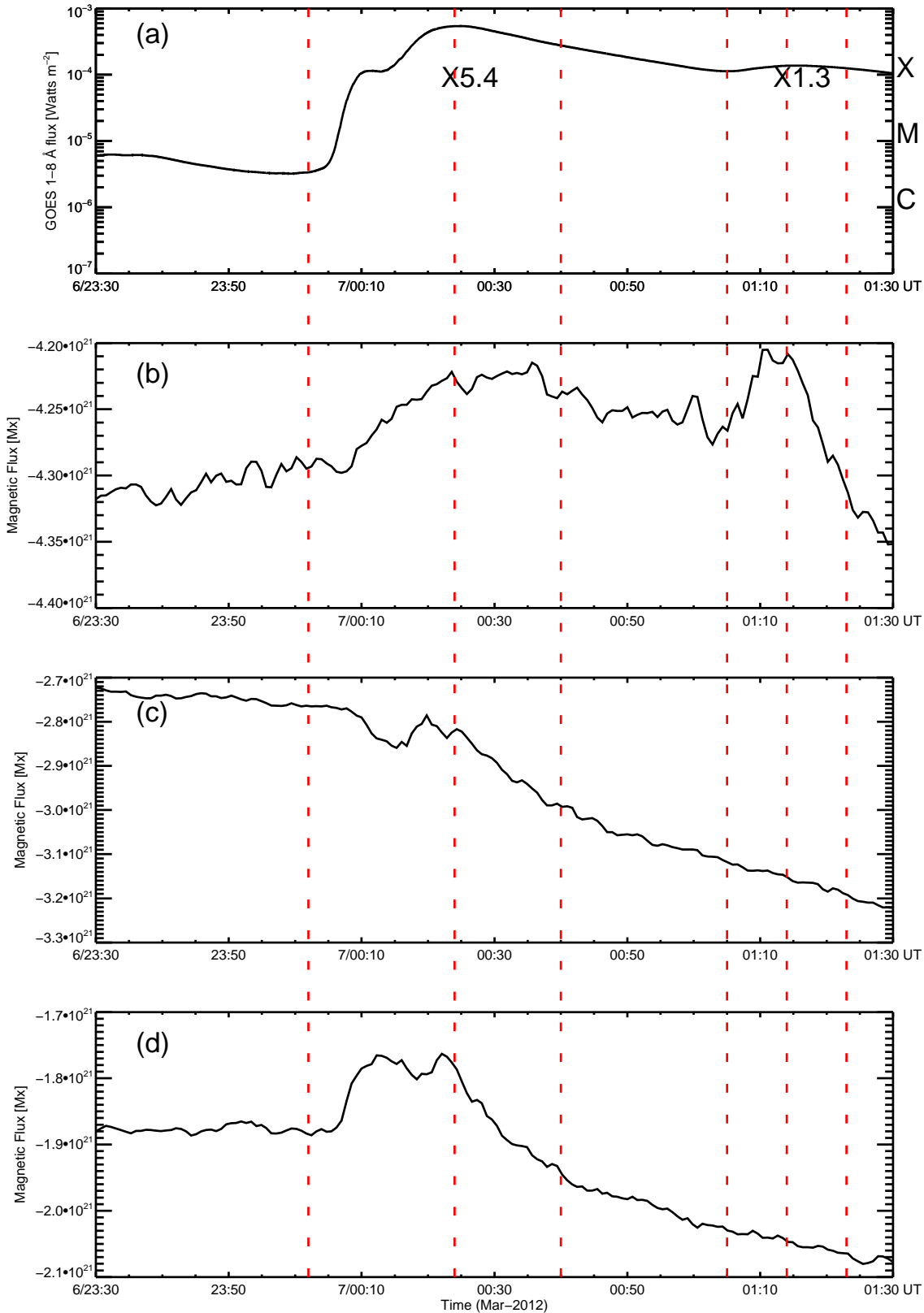


Fig. 7 Magnetic flux of sunspot N1, N2 and N3. (a) Evolution of GOES soft X-ray emission from 23:30 UT on 6 March to 01:30 UT on 7 March. The vertical dash lines represent the GOES flare start, peak and end times. (b)–(d) Time profiles of magnetic flux of sunspot N1, N2 and N3, respectively.